

Electrocatalytic Activity of Metal-Loaded Reticulated Vitreous Carbon Electrodes for Hydrogen Evolution from Flowing Alkaline Solutions

Mahmoud M. Saleh,*,† Maher H. El-Ankily, Mohamed S. El-Deab, and B. E. El-Anadouli

Department of Chemistry, Faculty of Science, Cairo University, Cairo, Egypt

Received December 7, 2005; E-mail: mahmoudsaleh90@yahoo.com

Reticulated vitreous carbon (RVC) electrodes have been used as possible porous cathodes, operating in flow-through mode for the purpose of the electrolytic generation of hydrogen gas from flowing alkaline solutions. The electrocatalytic performance of the RVC cathode was tested under different operating conditions, such as electrolyte flow regimes and temperature. Also, the effect of electroplating the RVC with copper metal or Watts nickel in flowing electrolytes has been assessed. Potentiodynamic and galvanostatic techniques along with SEM images were used to investigate the performance of the different cathodes: bare (uncoated) RVC, copper-coated RVC (RVC/Cu), and Ni-coated RVC (RVC/Ni). The hydrogen evolution reaction (HER) was found to be enhanced by coating RVC either with Cu or Ni. Polarization behavior had higher rates for HER using RVC/Ni than using RVC/Cu or bare RVC. This trend was confirmed by using a planar glassy carbon electrode (GC) coated with Cu and Ni under the same conditions. The activation energies for HER using RVC and RVC/Ni were estimated to be 32 and 14 kJ mol^{-1}, respectively. Current transient and SEM micrographs showed good electrocatalytic and mechanical stability of the metal loadings. There was no indication of loss of the catalytic properties after operation for 30 h. Model calculations helped to extract kinetic parameters for the HER using different electrodes.

Three-dimensional electrodes made of reticulated vitreous carbon (RVC) have been used in many applications, such as flow reactors.[1,2] This system offers several structural and operational advantages including a high area/volume ratio, i.e., high specific surface area, high porosity, high conductivity, and chemical and electrochemical stability. As well, they can be machined easily and have reasonable electrocatalytic properties. RVC electrodes may also be useful for the destruction of organic wastes[3,4] and removal of heavy metal ions from dilute streams.[5–7] In order to improve the performance and efficiency of the electrodes, the RVC is often modified and in fact, RVC electrodes coated with conductive polymers showed better electrocatalytic properties towards the removal of metal ions from dilute streams.[8]

The production of pure hydrogen is important both for potential industrial and energy storage applications. The development of reliable and cost effective technologies for the production of pure hydrogen is a challenging issue from electrochemical engineering point of view. For instance, for the H_2–O_2 operating fuel cells, ultra pure hydrogen gas (as a fuel) is a prerequisite. For hydrogen production from alkaline solutions, the cathodes that are used must have high stability, high specific surface area, and good electrocatalytic properties.[9–11] Nickel metal is currently used as a cathode for water electrolyzers due to its high electrocatalytic activity towards the hydrogen evolution reaction (HER). Different procedures were introduced to prepare nickel electrodes with high specific surface areas. These include sintering micro porous nickel,[12] production of nanoporous Raney-Nickel,[13] and incorporation of Ni into PolyHIPE polymer (PHP) matrix.[14] A nickel-loaded RVC matrix should be a very good porous cathode for the HER in flowing electrolytes. Porous electrodes have been used in hydrogen production[15,16] as well as in other industrial and environmental applications.[17–20] Three-phase (solid–liquid–gas) porous electrodes could be a special category of porous electrodes in which several operating parameters inherently control the electrodes overall performance. Of particular importance, the gas bubbles that are evolved accumulate inside the porous matrix resulting in non-uniform distributions of potential and current and, hence, in a lower effectiveness factor of the porous electrode.[21] Optimizing the electrolyte flow rate by other structural and transport parameters plays an important role in maximizing the performance of three-phase porous electrodes. Mathematical modeling can help to simulate the effects of different operating parameters on such systems.

The present work aims to study the performance of RVC and metal-coated RVC for electrocatalytic production of hydrogen gas from flowing alkaline solutions. The effect of the incorporation of Cu or Watts Ni (through electrodeposition) onto the RVC matrix towards the enhancement of the electrocatalytic performance of the RVC cathodes towards the HER was investigated. The results are compared with those of planar glassy carbon electrode (GC) coated with Cu and Ni in a stationary KOH electrolyte. A mathematical model is reviewed and applied to predict the behavior of the porous electrode and to extract kinetic parameters of HER for different candidate cathodes. The performance and stability of the different cathodes are evaluated.

† Present address: Department of Electronic Chemistry, Tokyo Institute of Technology, 4259 Nagatsuta, Midori-ku, Yokohama 226-8502

Published on the web November 9, 2006; doi:10.1246/bcsj.79.1711

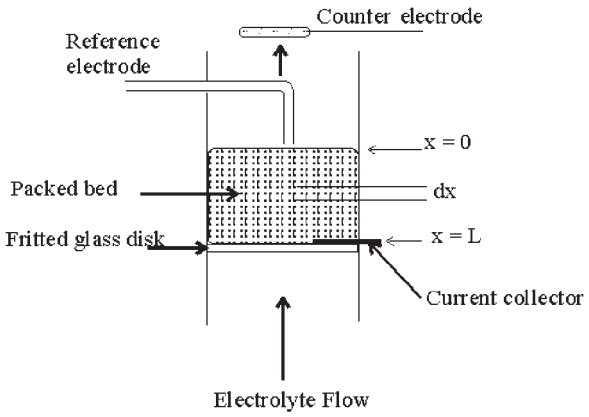

Fig. 1. Cell arrangement and flow direction.

Experimental

Materials and Methods. RVC blocks were supplied by Electrosynthesis Co., Inc. (New York) and were used as received. They had a specific surface area (S) equals 70 $cm^2\,cm^{-3}$ (i.e., cm^{-1}) and porosity (θ) of 0.90. They were cut in cylinders to fit the chamber of the packed bed electrode. The electrode had a diameter of 1.0 cm and an ohmic resistance < 0.01 ohm. The counter electrode was made of a platinum screen and was placed on the down-stream side of the porous electrode (Fig. 1). The reference electrode was of the type Hg/HgO/1 M KOH (having an equilibrium potential of 0.098 V vs NHE[22]). The potential reported here is that at the exit face relative to the down-stream reference electrode (denoted as E). Current densities are reported on the basis of the geometrical cross sectional area of the electrode (0.80 cm^2). A glassy carbon electrode (GCE) electrode of diameter 3.0 mm (from BAS Inc, Japan) was used in the planar electrode measurements. A conventional three-electrode cell was used in this case. Prior to the measurements, the GCE was polished first with emery paper (No. 2000), and then with aqueous slurries of successively finer alumina powder (particle size down to 0.06 μm) with the help of a polishing microcloth. The bare GCEs were then sonicated for 10 min in Milli-Q water.

An EG&G potentiostat/galvanostat, model 273A controlled by m352 electrochemical software was used in all measurements. The solutions were prepared by dissolving the desired weights of analytical grade KOH in doubly distilled water. The solution was circulated using a variable speed pump, and the flow rate was measured using volumetric measurements. The SEM micrographs were taken on a JEOL JSM-20 Scanning Electron Microscope. Further details of the experimental setup could be found elsewhere.[23]

Electroplating Procedure. Electroplating of the RVC porous matrix was performed in situ with copper or Watts nickel using flowing electroplating solutions. The electrode arrangement was described above (Fig. 1). The electroplating solutions and conditions are listed in Table 1.[24] The electroplating solutions were circulated for 1 h at a linear flow rate of 1.0 $cm\,s^{-1}$. However, because of the non-uniform distributions of the metal depositions within the porous matrix, we used RVC block of thickness equals 1.7 cm, and after the electroplating process, the last 0.7 cm at the back of the electrode was disregarded. The remaining 1.0 cm (near to the polarized face) had almost uniform distributions of the metal loadings. It was used as is or cut as required to only 0.5 cm. The problem of non-uniform distributions of metal currents and hence metal depositions within porous electrodes is well documented.[25,26] After electroplating, the blocks were rinsed with flowing water to remove all contaminants from the electrode chamber and from the blocks. Measurements were performed immediately after the cleaning process. An estimation of the extent of metal loading onto the RVC was done using Faraday's law. Assuming 100% current efficiency, the loading of Cu and Ni was found to be 95 and 88 $mg\,cm^{-3}$, respectively. Figures 2a–2c show

Table 1. Bath Compositions and Operating Conditions for Cu and Ni Electroplating on RVC and GC Electrodes

Metal	Bath composition /g L^{-1}		c.d. /mA cm^{-2}	Duration /h
RVC/Cu	$CuSO_4$	150	100	1
	H_2SO_4	50		
RVC/Ni	$NiCl_2$	25	100	1
(Watts Nickel)	$NiSO_4$	90		
	H_3BO_3	60		

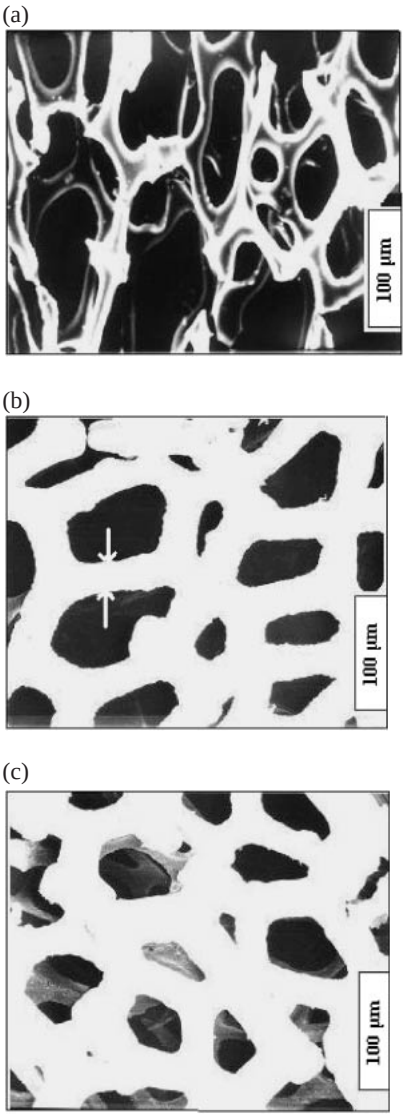

Fig. 2. SEM micrographs of the different electrodes a) bare RVC, b) RVC/Cu, and c) RVC/Ni. The white zones are the matrix. The arrows in Fig. 2b refer to a thread.

SEM micrographs of bare RVC, RVC/Cu, and RVC/Ni, respectively. The bright zones are the matrix, and the black zones are the voids. It is clear from the micrographs that the white zones are more pronounced in the case of the RVC/Cu or RVC/Ni due to metal depositions within the porous RVC matrix. The average thread diameter (see arrows in Fig. 2b) of bare RVC, RVC/Cu, and RVC/Ni were estimated to be 17.86, 30.95, and 31.55 μm, respectively. This clearly reflects the effective electrodeposition of Cu and Ni onto the fibrous texture of the RVC matrix. A similar electroplating procedure for the planar GC electrode was conducted but from stationary solution and for a period of 30 s. This was enough to cover the GC with Cu or Ni.

Mathematical Model

The HER using porous RVC cathodes in flowing alkaline solutions is a typical representative example of a three-phase electrocatalytic reactor, in which gases are electrogenerated within the solid porous matrix of the cathode, initially filled with electrolyte. Hence, several disadvantages arose including a decrease in the pore electrolyte conductivity, a decrease in the effective real surface area of the porous matrix, and thus, an overall decrease in the performance of the cathode. In this section, a previously developed mathematical model is reviewed.[21] Electrocatalytic gas evolution is a significant and complicated phenomenon in electrochemical systems from both academic and engineering view points. The generation of gas bubbles in the reaction medium strongly affects the pore electrolyte resistivity and, hence, on the overall performance of the system. Therefore, it is necessary to evaluate the effects of the gas bubbles on the overall polarization behavior of the electrode and on the current and potential distributions. When gas is evolved within a porous electrode, the conducting medium is heterogeneous mixture of three phases, i.e., solid porous electrode, liquid aqueous electrolyte, and gas bubbles. The geometry of the interfaces and the conducting medium within the porous electrode is complicated and difficult to predict. Since the rate of generation of gas bubbles is rather non uniform within the porous electrode, the gas void fraction, $\in$, and the pore electrolyte conductivity, κ, are also non uniform within the electrode. The porosity of the packed bed is uniform throughout the electrode, and therefore, the variation in pore electrolyte conductivity is related to the variation in the gas void fraction.

Figure 1 shows the arrangement of the porous electrode and the direction of the electrolyte flow. In developing the model, the following assumptions were made.[21] Butler–Volmer equation controls the rate of charge-transfer reaction, which involves a one-electron-transfer rate-determining step. The porous electrode is assumed to be inert substrate and does not anodically dissolve under the present conditions. The potential gradient within the solid phase of the packed bed can be neglected due to its high conductivity compared to the electrolyte. It is characterized by a uniform porosity, θ, and a specific surface area, S ($cm^2\,cm^{-3}$). Finally, ionic migration effects are negligible.

Butler–Volmer equation[21] correlates the solution current density, $i(x)$ with the polarization by

$$\frac{di(x)}{dx} = -J(x) = \frac{-i_{o,H}S[1 - \exp(\eta(x)/b)]}{\exp(\alpha\eta(x)/b)}, \quad (1)$$

where $J(x)$ is the reaction current per unit reaction volume ($A\,cm^{-3}$). The other variables are listed in the notation section. Ohm's law relates the solution current travels through the gas-electrolyte dispersion filing the pore space with the change in polarization. Therefore,

$$i(x) = \kappa(x)\frac{d\eta(x)}{dx}. \quad (2)$$

The conductivity of the gas-electrolyte dispersion within the pores, $\kappa(x)$, is a complex function that depends on composition of the electrolyte, the porosity, and $\in$. The latter varies with the distance within the electrode following the variation of $i(x)$ which generates the gas bubbles. Bruggeman's equation is used to correlate the conductivity of the gas-electrolyte dispersion which fills the pore space with the gas void fraction,[27] i.e.,

$$\kappa(x) = \kappa^o[\theta - \in(x)]^{3/2}, \quad (3)$$

where κ^o is the bulk electrolyte conductivity ($ohm^{-1}\,cm^{-1}$) and $\in(x)$ is the gas void fraction, which is given by[19]

$$\in(x) = \frac{\theta i(x)}{Q\gamma + i(x)}, \quad (4)$$

where γ is a conversion factor of the current to the volume of the generated gas. Assuming ideal gas behavior, γ is given by

$$\gamma = \frac{2PF}{RT}, \quad (5)$$

where γ equals $7.87\,C\,cm^{-3}$ for hydrogen evolution reaction at standard pressure and temperature.[19]

The boundary conditions are:

$$\begin{aligned} &x = 0, \quad i = i_{cell} \\ &x = L, \quad i = 0 \quad d\eta/dx = 0 \quad \kappa = \kappa^o\theta^{1.5} \quad \text{and} \quad \in = 0 \end{aligned} \quad (6)$$

A system of four equations (Eqs. 1–4) describes the distributions of four variables, i.e., i, η, $\in$, and κ are obtained. The above system of equations was solved using a numerical technique developed by Newman.[28] The present theoretical framework was used to predict the polarization behavior of the porous electrode, to fit the experimental data with the model predictions and to estimate some kinetic parameters such as the exchange densities of the HER for different electrodes.

Results and Discussion

Electrolyte Flow Rate. The significance of the bubble formation within the porous matrix was studied by allowing the bubbles to build up at stationary conditions ($Q = 0$) at a known generation rate, and the potential response was recorded. This was done by measuring potential–time relation for the HER using bare RVC with a thickness (L) of 1.0 cm in 2 M KOH. The current was fixed at $200\,mA\,cm^{-2}$, and the potential measured under stationary conditions, (i.e., $Q = 0$). As shown in Fig. 3, the potential increases with time until it reaches a plateau after about 30 min. The time period depends on the transport and structural parameters of the system under investigation. When $Q = 1.0\,cm\,s^{-1}$ (point "a" in the figure), the potential decreases sharply from −2.6 to −2.25 V with respect to the reference electrode. When $Q = 0$, bubbles accumulate in the pores of the electrode, and they fully occupy the void fraction.[29] The experimental potential difference, ΔE_{exp} between

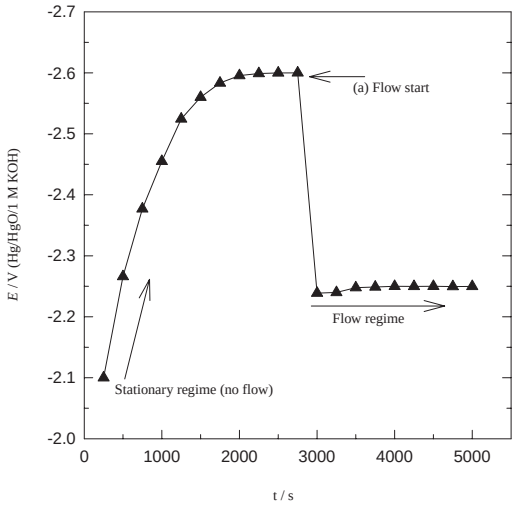

Fig. 3. Potential–time relations at different flow regimes for HER on bare RVC at cell current $= 0.2\,\mathrm{A\,cm^{-2}}$ and 25 °C.

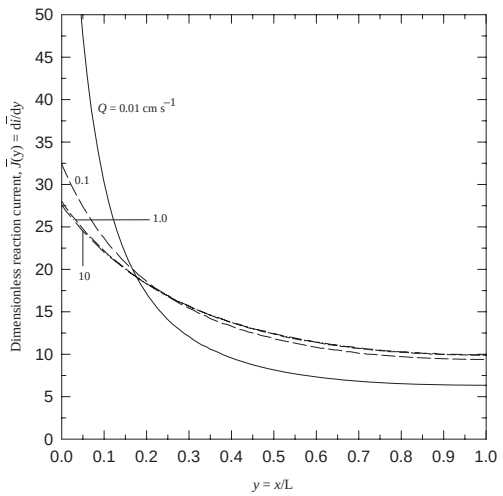

Fig. 4. Theoretical results of the distributions of the dimensionless reaction current of the HER on bare RVC at different Q. $L = 1\,\mathrm{cm}$ and $[\mathrm{KOH}] = 2\,\mathrm{M}$.

the stationary and the flowing regimes, which are shown in Fig. 3, at this current density is:

$$\Delta E_{\mathrm{exp}} = E_{Q=0} - E_{Q=1} \approx 0.35\,\mathrm{V}, \tag{7}$$

where $E_{Q=0}$ is the electrode potential at stationary regime and $E_{Q=1}$ is the potential at $Q = 1\,\mathrm{cm\,s^{-1}}$ and current density $= 200\,\mathrm{mA\,cm^{-2}}$. The ΔE_{exp} is a function of the system parameters, and mathematical modeling must be used to account for the effects of gas bubble formation on the behavior of porous electrode.

It has been shown before that Q has a dramatic effects on the distributions of $\in(x)$ and $\kappa(x)$.[21,23] As the gas void fraction increases, the pore electrolyte conductivity decreases according to Eq. 3. This causes non-uniform polarization and current distributions within the porous electrode. Figure 4 shows theoretical results of the effects of Q on the distributions of the dimensionless reaction current, $\bar{J}(y)$ of HER using the parameters shown in Table 2. The values of $\bar{J}(y)$ were taken as

Table 2. Parameters Used in Production of the Theoretical Results in Figs. 4 and 5 and in Fitting the Experimental Data in Fig. 6

$S = 70\,\mathrm{cm^2\,cm^{-3}}$
$L = 1.0\,\mathrm{cm}$
$\alpha = 0.35$
$[\mathrm{KOH}] = 2\,\mathrm{M}$
$\kappa^{\mathrm{o}} = 0.25\,\Omega^{-1}\,\mathrm{cm^{-1}}$
$\theta = 0.90$
$i_{\mathrm{o,H}} = 2 \times 10^{-4}\,\mathrm{A\,cm^{-2}}$ (bare RVC)

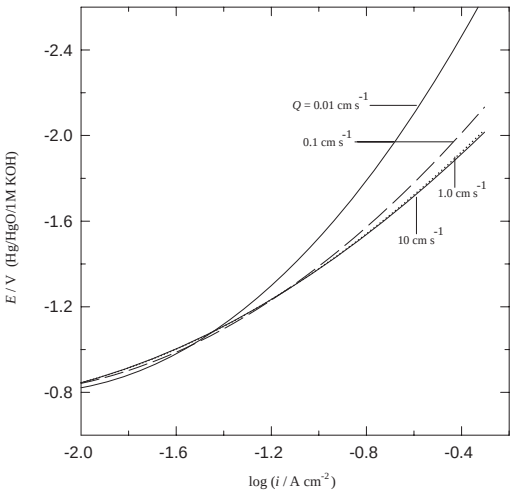

Fig. 5. Theoretical results of the i–E relations of HER on bare RVC at different flow rate, Q. $L = 1\,\mathrm{cm}$ and $[\mathrm{KOH}] = 2\,\mathrm{M}$.

$J(x)/i_{\mathrm{o,H}}S$ and the dimensionless distance, y was equal to x/L. At lower Q values, i.e., $Q \leq 0.01\,\mathrm{cm\,s^{-1}}$, gas bubble formation is significant and results in an increase in $\in$ and hence, a decrease in κ. This is in accordance with Eqs. 3 and 4. As a result, the potential and, hence, the current becomes more non-uniform.[21,23] As Q increases, the reaction current becomes more uniform. At higher values of Q, the bubbles are swept out of the porous matrix and, consequently, the bubble effects are minimum. Therefore, the polarization and current distributions become more uniform.

Figure 5 shows the polarization curves simulated from the model calculations at the same Q used in Fig. 4. As Q increases, the polarization lines shifted to higher currents at the same values of polarization, and the degree of $\in(x)$ decreases while $\kappa(x)$ increases. Accordingly, the polarization required to obtain definite reaction rates (current densities) decreases. Also, as the conductivity increases, the polarization becomes more uniform, and a higher utility of the bed was obtained. There are no differences in polarization between $Q = 1.0$ and $10\,\mathrm{cm\,s^{-1}}$. Under these conditions, $Q = 1.0\,\mathrm{cm\,s^{-1}}$ is enough to reduce the effects of the gas bubbles using the present system parameters. Similar curves were calculated at KOH concentrations of 1 and 3 M, and the same results were obtained. The above results showed that $Q = 1.0\,\mathrm{cm\,s^{-1}}$ is good for operating the present gas evolving flow-through porous electrode.

Metal Loadings. Metal loading onto RVC were carried out as described in the experimental section. Figure 6 shows

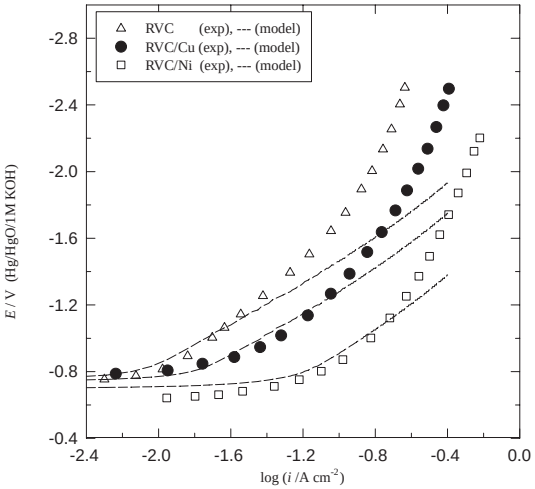

Fig. 6. *i–E* relations for HER from 2 M KOH on different electrodes at $Q = 1\,\mathrm{cm\,s^{-1}}$, $L = 0.5\,\mathrm{cm}$ at 25 °C. The dashed lines are the model calculations and the symbols are the experimental data.

i–E relations for the HER on bare RVC, RVC/Cu, and RVC/Ni in 2 M KOH at $Q = 1\,\mathrm{cm\,s^{-1}}$ at 25 °C. The symbols represent the experimental data, and the lines represent predicted values. First, the experimental data were fitted with the model calculations for the HER on bare RVC in 2 M KOH using a value of α equals 0.35 and exchange current density $i_{o,H}$ equals $2 \times 10^{-4}\,\mathrm{A\,cm^{-2}}$. The experimental data of RVC/Cu and RVC/Ni were then fitted only by using $i_{o,H}$ as the fitting parameter. The rest of parameters used in the model calculations are the same as those listed in Table 2 but with $L = 0.5\,\mathrm{cm}$. Comparison of the model predictions satisfactorily agrees with the experimental results at low and moderate rates of gas evolution. However, at higher current densities, the model predicts lower polarizations. This was attributed to the trapped gas bubbles inside the pores of the matrix. Also, the model should be modified in the future to account for the surface coverage by gas bubbles. The fitted values of $i_{o,H}$ on RVC, RVC/Cu, and RVC/Ni were 2×10^{-4}, 4×10^{-4}, and $1.5 \times 10^{-3}\,\mathrm{A\,cm^{-2}}$, respectively. These values are comparable with the literature values.[30] The model and the experimental results conclude that the potentials required to obtain certain current densities (i.e., rates of HER) decrease in the order:

$$\mathrm{RVC/Ni} < \mathrm{RVC/Cu} < \mathrm{RVC}. \quad (8)$$

The above trend was confirmed by using a planar GC electrode instead of the porous RVC electrode. Data for the HER in nonflowing 2 M KOH using GC, GC/Cu, and GC/Ni electrodes were recorded as shown in Fig. 7. Better electrocatalytic activity toward the HER was obtained with GC/Ni than with GC/Cu or bare GC. Note that the values of the reversible electrode potential, E_H, in both cases, i.e., RVC (Fig. 6) and GC (Fig. 7) electrodes, are closer, and both are comparable with the theoretical value. The theoretical value of E_H can be calculated from the relation: $E_H = -0.0591x\mathrm{pH}$ as -0.83 V (NHE). The above results imply that the RVC/Ni and RVC/Cu electrodes have enhanced electrocatalytic properties for the HER than that of RVC. These were attributed to the electrocatalytic properties of Ni and Cu as well as the roughness of Ni and Cu coatings, which increase the true surface area of the porous RVC matrix.

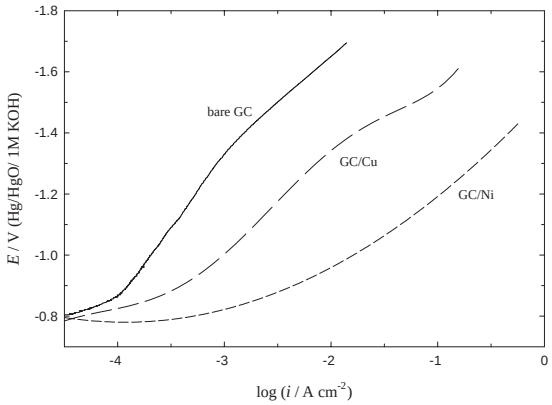

Fig. 7. *i–E* relations for HER in 2 M KOH with planar GC, GC/Cu, and GC/Ni electrodes at 25 °C.

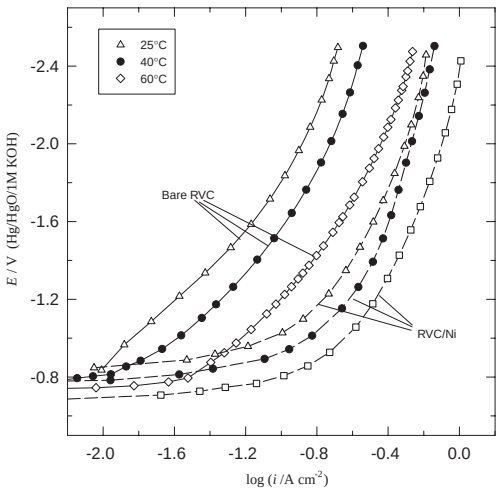

Fig. 8. Experimental data of *i–E* relations for HER in 2 M KOH with bare RVC (solid lines) and RVC/Ni (dashed lines) at $Q = 1\,\mathrm{cm\,s^{-1}}$, $L = 0.5\,\mathrm{cm}$ at different temperatures.

Effects of Temperature. Figure 8 illustrates the effects of temperature on the current–potential relations of HER in 2 M KOH with RVC and RVC/Ni. The results of RVC/Ni electrode are introduced only because they are interesting, and no model studies are introduced here since the effects of temperature on such systems require that the model be modified. As the temperature increases, the cathodic potential, i.e., the power consumption, required to attain specific rates of HER decreases. At a given potential, an increase in temperature leads to an increase in the current density. The effects of temperature on the *i–E* relations can be attributed to two primary factors. The conductivity of the electrolyte and the rate of charge transfer at the electrode/electrolyte interface increase with temperature. A secondary factor may arise due to the effects of temperature on the surface tension and viscosity of the electrolyte and, hence, on the bubble size, which, in turn, affects the pore electrolyte resistively. While an increase in the conductivity of the electrolyte leads to a decrease in the ohmic potential drop in the pore electrolyte, the increase in

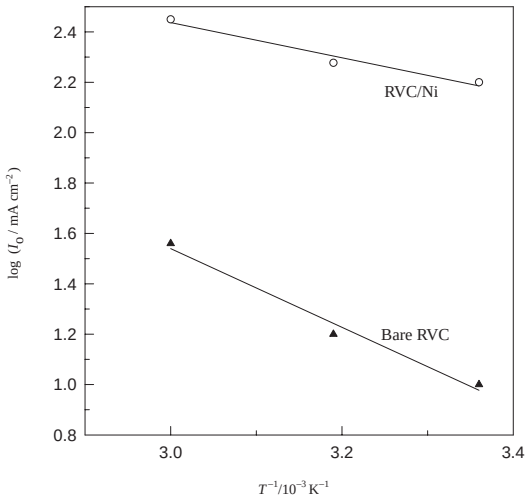

Fig. 9. Arrhenius plots of the HER with RVC and RVC/Ni. The same parameters as in Fig. 7 are used.

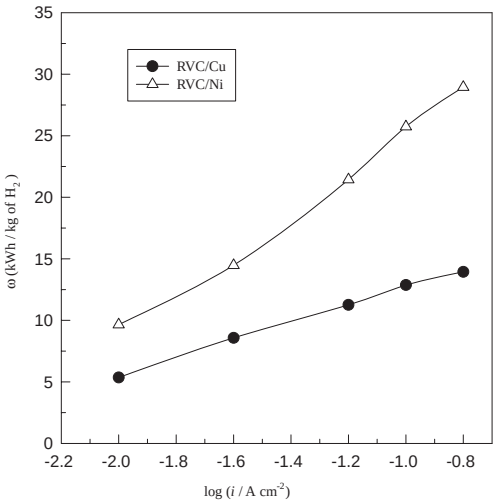

Fig. 10. Power savings for the HER on both RVC/Cu and RVC/Ni. The same parameters as in Fig. 6 are used.

temperature leads to an increase in $i_{o,H}$ of the hydrogen evolution reaction and hence to a decrease in the activation polarization. Consequently, at relatively high temperatures the activation and ohmic polarization associated with the HER are lower, and thus, power consumption is lower.

The apparent total exchange current density per geometrical surface area, I_o, can be estimated by extrapolating cathodic Tafel line to the equilibrium potential.[31,32] This can be done with the *i–E* relations shown in Fig. 8 for the HER with bare RVC and RVC/Ni. Using this method the values of I_o are estimated for the two electrodes at different temperatures. The values of I_o are only apparent values and may have some error, since the current and the polarization are not completely uniform.[33,34] The apparent activation energy, E_a for the HER reaction can then be estimated from the temperature dependence of I_o using Arrhenius equation;[31,35]

$$E_a = -R\left[\frac{\partial \ln I_o}{\partial(1/T)}\right], \tag{9}$$

where R is the gas constant. A plot of $\log I_o$ vs $1/T$ gives a straight line from which the slope can be used to determine E_a. Arrhenius plots for the bare RVC and RVC/Ni are shown in Fig. 9. The estimated values of E_a are found to be 32 and 14 kJ mol^{-1}, for bare RVC and RVC/Ni, respectively. The results showed that modification of RVC cathodes by coating RVC with Ni reduces the apparent activation energy of the HER. The reduction in E_a for RVC/Ni is pronounced which indicates that the HER with RVC/Ni is more facile than on RVC.

Energy Savings. The decrease in the polarization when RVC was coated with Cu or Ni, as shown in Fig. 6, was further analyzed. The energy saving in watt hours, $\Delta\xi$, at the cathode at a particular current, i is given by

$$\Delta\xi = \frac{i\Delta Et}{3600}, \tag{10}$$

where t is the electrolysis time in seconds, ΔE is the lowering in the cathodic polarization (in Volt) at a particular current, i (in Ampere) at the cathode due to Cu or Ni loading. The values of ΔE were calculated from the collected *i–E* relations for the HER in 2 M KOH using $L = 0.5$ cm. The data were drived from Fig. 6. This was done by subtracting the potentials for RVC from that of RVC/Cu or RVC/Ni at the same current densities. The amount of hydrogen gas produced in gram equivalent is given by Faraday's law as it/F. Consequently, the energy savings, ω, at the cathode in kW h per kilogram of hydrogen gas is given by,

$$\omega = \frac{i\Delta E(t/3600)}{i(t/F)} = \frac{\Delta EF}{3600}. \tag{11}$$

The values of ω were calculated at different current densities and plotted against the current density as shown in Fig. 10. ω per kilogram of hydrogen gas increases with the increase in the operating cell current, and its values are more pronounced for the RVC/Ni electrode. Significant differences begin to appear at high operating cell currents which are of practical interest for water electrolysis.

Stability of Cu and Ni Coatings. The results discussed so far showed that Cu and Ni coatings enhanced the rate of HER both at lower and relatively higher temperatures. This was attributed to the good electrocatalytic properties due to metal loading. However, the stability of these coatings is of primary importance. The stability was determined by holding the potential at -2.0 V and measuring current–time relations for both coatings. It was found that the current dropped in the first few minutes to lower values and remained constant for a period of about 30 h for both electrodes metal loaded. These results implied that there was no surface failure for either RVC/Cu or RVC/Ni. This period might be too short; however, it is reasonable for the purpose of the present study. The stability of the metal coatings was also examined by SEM micrographs before and after the above period of operation. The micrographs are shown in Figs. 11a and 11b for Cu and Ni coatings, respectively. A comparison between the micrographs of RVC/Cu and RVC/Ni before (Figs. 2b and 2c) and after (Figs. 11a and 11b), operation for this period indicates that the metal dispersions are mechanically stable. A lower degree of metal loadings on the used electrodes (Figs. 11a and 11b) could be seen from the micrographs, and this was attributed to the removal of

(a)

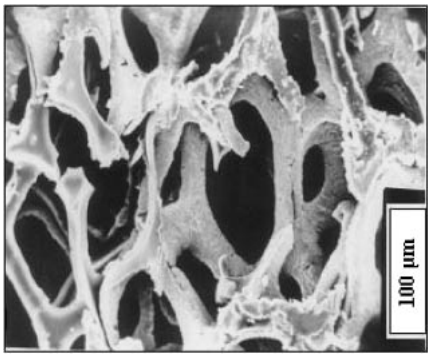

(b)

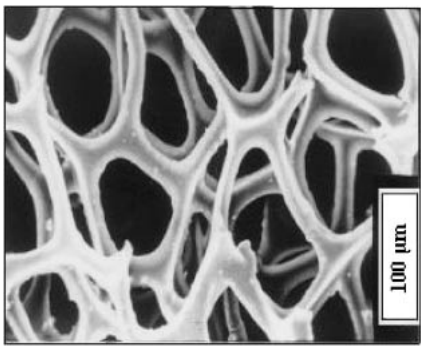

Fig. 11. SEM micrographs of the different electrodes: (a) RVC/Cu and (b) RVC/Ni after an operation period of 30 h of HER at −2.0 V. The white zones are the matrix.

excess deposited metal (weak adhesion) which probably flaked off in the electrolyte streams. This may occur the first few minutes concurrent with the decrease in the initial current decrease as stated above. A slight thinning of the average wire diameter down to 20.83 and 21.43 μm is observed after prolonged operation of the RVC/Cu and RVC/Ni electrodes, Figs. 11a and 11b, respectively. This fact reflects the loss of some of the Cu and Ni from the fibrous matrix of the RVC electrodes, while having a relatively thicker average wire diameter compared to the bare RVC. The coatings remain adhered for long time thus have the required performance and stability. Electroplating for less than one hour is enough for the present investigation.

Summary and Conclusion

The present study evaluated the possibility of modifying the RVC electrodes by loading metal dispersions onto the porous matrix. A mathematical model helped to understand the effects of Q on the overall behavior of the porous electrode and on the potential and current distributions of the HER within the electrode. It was also possible to extract the exchange current density of the HER using different electrodes. Disagreements between the calculated values and the experimental data occurred at higher current densities. RVC/Cu and RVC/Ni have better electrocatalytic properties towards the HER than the bare RVC, and this trend was confirmed by comparison with a planar GC electrode instead of the RVC. Current-transient and SEM micrographs showed that the RVC/Cu and RVC/Ni electrodes are stable. The power savings due to metal loading were evaluated. The model must be further modified to account for surface coverage by gas bubbles.

References

1 J. M. Friedrich, C. P. de-Leon, W. Reads, F. C. Walsh, *J. Electroanal. Chem.* **2004**, *561*, 203.
2 E. L. Gyenge, C. W. Oloman, *J. Appl. Electrochem.* **2003**, *33*, 665.
3 R. Hozle, A. M. L. Castro, *J. Appl. Electrochem.* **1988**, *18*, 679.
4 A. A.-Gallegos, D. Pletcher, *Electrochim. Acta* **1999**, *44*, 2483.
5 M. Maltoz, J. Newman, *J. Elecrochem. Soc.* **1986**, *133*, 1850.
6 J. Wang, H. D. Dewald, *J. Elecrochem. Soc.* **1983**, *130*, 1814.
7 R. C. Windner, M. F. B. Sousa, R. Bertazzoli, *J. Appl. Electrochem.* **1998**, *28*, 201.
8 C. M. S. Piatnicki, D. S. Azambuja, E. E. S. Hasse, K. R. L. Castagno, S. B. Guterres, *Sep. Sci. Technol.* **2002**, *37*, 2459.
9 I. A. Raj, *Appl. Surf. Sci.* **1992**, *59*, 245.
10 D. L. Stojić, M. P. Marčeta, S. P. Sovilj, Š. S. Miljanić, *J. Power Sources* **2003**, *118*, 315.
11 M. Treuba, S. Trasatti, S. Trasatti, *Mater. Chem. Phys.* **2005**, in press.
12 O. Böhme, F. U. Leidich, H. J. Salge, H. Wendt, *Int. J. Hydrogen Energy* **1994**, *19*, 349.
13 S. Rausch, H. Wendt, *J. Electrochem. Soc.* **1996**, *143*, 2852.
14 I. J. Brown, S. Sotiropoulos, *J. Appl. Electrochem.* **2000**, *30*, 107.
15 M. S. El-Deab, M. M. Saleh, *Int. J. Hydrogen Energy* **2003**, *28*, 1199.
16 V. D. Stankovic, R. Grujic, A. A. Wragg, *J. Appl. Electrochem.* **1998**, *28*, 321.
17 M. R. V. Lanza, R. Bertazzoli, *J. Appl. Electrochem.* **2000**, *30*, 61.
18 F. Coeuret, V. E. Oliveira, C. E. Bezerra, *J. Appl. Electrochem.* **2002**, *32*, 1175.
19 J. Newman, W. Tiedman, *Flow-through Porous Electrodes*, ed. by H. Gerischer, C. W. Tobias, in *Advances in Electrochemistry and Electrochemical Engineering*, ed. by H. Gerischer, C. W. Tobias, Wiley, New York, **1978**, Vol. 11, pp. 352–438.
20 R. E. Sioda, K. B. Keating, in *Electroanalytical Chemistry*, ed. by A. J. Bard, Marcel Dekker Inc., New York, **1982**, Vol. 12.
21 M. M. Saleh, *J. Phys. Chem. B* **2004**, *108*, 13419.
22 D. Dobos, *Electrochemical Data*, Elsevier, New York, **1975**, p. 242.
23 B. G. Ateya, B. E. El-Anadouli, J. W. Weidner, M. M. Saleh, *J. Elecrochem. Soc.* **1995**, *142*, 4122.
24 O. N. Tandon, V. K. Aggarwal, K. C. Dhinga, *Handbook of Electroplating and Anodization*, Delhi, **1981**, p. 181.
25 J. A. Trainham, J. Newman, *J. Electrochem. Soc.* **1977**, *124*, 1528.
26 R. Alkire, B. Gracon, *J. Electrochem. Soc.* **1975**, *122*, 1594.
27 R. E. Merdith, C. W. Tobias, *Conduction in Heterogeneous Systems*, in *Advances in Electrochemistry and Electrochemical Engineering*, ed. by H. Gerischer, C. W. Tobias, Wiley, New York, **1962**, Vol. 2, pp. 17–48.

28 J. Newman, *Electrochemical Systems*, 2nd ed., Prentice-Hall, Englood Cliffs, NJ, **1991**, p. 552.
29 M. M. Saleh, *Electrochim. Acta* **1999**, *45*, 959.
30 A. J. Appleby, M. Chelma, H. Kita, G. Bronoel, *Encyclopedia of the Electrochemistry of Elements*, ed. by A. J. Bard, Marcel Dekker, NY, **1982**, p. 556.
31 W.-X. Chen, *Int. J. Hydrogen Energy* **2001**, *26*, 603.
32 C. Hitz, A. Lasia, *J. Electroanal. Chem.* **2000**, *500*, 213.
33 B. G. Ateya, L. Austin, *J. Electrochem. Soc.* **1977**, *124*, 1528.
34 B. G. Ateya, *J. Electroanal. Chem.* **1977**, *75*, 183.
35 H. J. Miao, D. L. Piron, *Electrochim. Acta* **1993**, *38*, 1079.